NeuroImage 82 (2013) 326–335

Contents lists available at ScienceDirect

NeuroImage

journal homepage: www.elsevier.com/locate/ynimg

Time-on-task and sleep deprivation effects are evidenced in overlapping brain areas ☆

Christopher L. Asplund, Michael W.L. Chee *

Centre for Cognitive Neuroscience, Neuroscience and Behavioral Disorders Program, Duke-NUS Graduate Medical School, Singapore, Singapore

ARTICLE INFO

Article history:
Accepted 26 May 2013
Available online 6 June 2013

Keywords:
Sleep deprivation
Time-on-task
Attention
Arterial spin labeling
BOLD fMRI

ABSTRACT

Both sleep deprivation and extended task engagement (time-on-task) have been shown to degrade performance in tasks evaluating sustained attention. Here we used pulsed arterial spin labeling (pASL) to study participants engaged in a demanding selective attention task. The participants were imaged twice, once after a normal night of sleep and once after approximately 24 h of total sleep deprivation. We compared task-related changes in BOLD signal alongside ASL-based cerebral blood flow (CBF) changes. We also collected resting baseline CBF data prior to and following task performance. Both BOLD fMRI and ASL identified spatially congruent task activation in ventral visual cortex and fronto-parietal regions. Sleep deprivation and time-on-task caused a decline of both measures in ventral visual cortex. BOLD fMRI also revealed such declines in fronto-parietal cortex. Only early visual cortex showed a significant upward shift in resting baseline CBF following sleep deprivation, suggesting that the neural consequences of both SD and ToT are primarily evident in task-evoked signals. We conclude that BOLD fMRI is preferable to pASL in studies evaluating sleep deprivation given its better signal to noise characteristics and the relative paucity of state differences in baseline CBF.

Introduction

The study of sustained attention and its decline with sleep deprivation (SD) and time-on-task (ToT) was first motivated by specific transport and military demands. The findings from this research have since gained broader appeal as more persons become part of the 24/7 global supply chains on which modern life depends. Sustained attention, one of the most severely and consistently affected cognitive domains following SD (Lim and Dinges, 2010), declines during extended task engagement. Resource models attribute this decline to the exhaustion of cognitive (Shaw et al., 2009; Warm et al., 2008) or neural (Doran et al., 2001) resources. Consistent with the notion that information processing capacity is reduced during SD (Kong et al., 2011, 2012), ToT effects have been shown to be more pronounced in sleep-deprived individuals (Van Dongen et al., 2011; Warm et al., 2008; Wilkinson, 1964). Such behavioral interactions suggest that SD and ToT may affect the same processing stages (additive factors logic; see Schweickert, 1985; Sternberg, 1969), and perhaps common neural pathways as well.

Functional imaging employing BOLD (Blood Oxygen Level Dependent) fMRI has provided insights into the neural underpinnings of the neurobehavioral deficits encountered during SD. Studies of preparatory attention (Chee et al., 2011), working memory (Bell-McGinty et al., 2004; Chee and Chuah, 2007; Habeck et al., 2004; Mu et al., 2005), and selective attention (Chee et al., 2010; Kong et al., 2012; Lim et al., 2010a; Tomasi et al., 2009) offer converging evidence for SD-related declines in task-evoked fronto-parietal activation. These decreases in BOLD signal are thought to result from reduced engagement of brain regions involved in the top-down control of attention (Corbetta and Shulman, 2002; Kastner et al., 1999), accompanied by reduced signal in their putative targets such as visual extrastriate cortex.

Resource theories of the ToT effect (Warm et al., 2008) predict decreases in neural activation and regional blood flow as one is engaged in a task over time. Accordingly, Transcranial Doppler Imaging has been used to demonstrate hemispheric reductions in cerebral blood flow velocity following sustained task performance (Shaw et al., 2009). However, the technique does not localize the brain regions responsible for the effect. Resource theories additionally predict that the brain regions showing ToT effects are the same ones engaged during task performance. Indeed, functional imaging studies using different modalities (arterial spin labeling (ASL), PET, NIRS, and BOLD fMRI) have demonstrated regionally specific ToT effects (Coull et al., 1998; Grant et al., 2009; Langner and Eickhoff, 2012; Lim et al., 2010b; Paus et al., 1997). To date, though, only one has investigated sleep-deprived persons. Furthermore, as these studies used different tasks, different combinations of altered parietal, frontal, and thalamic signal or blood flow have been reported (Coull et al., 1998; Grant et al., 2009; Langner and Eickhoff, 2012; Lim et al., 2010b; Paus et al., 1997). It is thus unclear whether SD and ToT effects occur in similar brain regions.

BOLD fMRI has been the dominant technique used in cognitive neuroscience because of its versatility and superior temporal and

☆ Funding acknowledgments: This work was supported by a grant awarded to Dr Michael Chee from the National Medical Research Council Singapore (STaR/0004/2008).

* Corresponding author at: Cognitive Neuroscience Laboratory, Duke-NUS Graduate Medical School, 8 College Rd, #06-18, Singapore 169857, Singapore. Fax: +65 62218625.
E-mail address: michael.chee@duke-nus.edu.sg (M.W.L. Chee).

1053-8119/$ – see front matter © 2013 Elsevier Inc. All rights reserved.
http://dx.doi.org/10.1016/j.neuroimage.2013.05.119

spatial SNR characteristics (Parrish et al., 2000). However, it has been proposed that investigations of vigilance and time-on-task effects might benefit from the greater temporal stability of arterial spin labeling (ASL) (Brown et al., 2007; Demeter et al., 2011; Lim et al., 2010b; Rao, 2012), which makes it well suited for studying gradual shifts in neural activity during continuous tasks (Aguirre et al., 2002; Wang et al., 2005). Unlike BOLD fMRI, which is a relative measure, ASL also provides a means to quantify cerebral blood flow (CBF) in physiological units (Buxton et al., 1998; Rao, 2012; Wong et al., 1997). This allows for the comparison of resting baseline CBF across sessions and states.

ASL and PET studies have identified regional CBF differences, both task-evoked and baseline, between SD and the well rested state (Braun et al., 1997; Poudel et al., 2012; Thomas et al., 2000; Wu et al., 1991, 2006). These state effects often represent CBF reductions during SD, but some regional increases have also been reported (Braun et al., 1997; Wu et al., 2006). One might expect similar BOLD findings, as BOLD and CBF signals are tightly coupled under normal circumstances (Hoge et al., 1999). However, under some conditions, such as those encountered during aging, this coupling may be altered so as to yield smaller BOLD signal changes during task performance (Ances et al., 2009; Bangen et al., 2009). If similar changes in vascular behavior occur during sleep deprivation, they may influence the interpretation of fMRI findings in studies involving sleep deprivation.

In the present experiment, we employed an fMRI sequence that allowed us to analyze both BOLD and ASL signals related to performing an extended attention-demanding task. Each participant completed the experiment when rested and again after a night of total sleep deprivation. This design allowed us to address three outstanding issues. First, we directly compared the neural correlates of sleep deprivation and time-on-task effects to determine if they spatially overlapped. Given our challenging task and the task breaks required for BOLD fMRI, we explored both short-term, within-run effects (Ong et al., in press; Temple et al., 2000) and long-term, between-run effects (Coull et al., 1998; Lim et al., 2010b; Paus et al., 1997). Second, we examined whether BOLD and CBF measures of task-related neural activity are congruent across the rested and sleep deprived states. A crucial issue to be addressed by the study is whether a reasonably long experiment using ASL and BOLD would result in agreement regarding how SD modulates task-related activation. Finally, we examined resting baseline shifts in CBF across state and time-on-task.

Materials and methods

Participants

Twenty members of the National University of Singapore (NUS) community (11 females, aged 22.2 +/− 2.7, mean +/− standard deviation) were studied after providing informed consent, in compliance with a protocol approved by the NUS Institutional Review Board. They were selected from respondents of a web-based questionnaire who (1) were right-handed, (2) had regular sleeping habits, (3) slept no less than 6.5 h/night, (4) were not on any long-term medications, (5) had no symptoms or history of psychiatric, neurological, or sleep disorders, (6) drank fewer than 3 caffeinated drinks per day, and (7) were not of an extreme chronotype as assessed by the Horne-Östberg Morningness-Eveningness questionnaire (Horne and Östberg, 1976), i.e. having a score between 35 and 65. All reported having normal or corrected-to-normal vision.

The participants' sleep habits were monitored throughout the duration of the study using motion-sensing wrist actigraphy (Actiwatch, Philips Respironics, USA). Only those whose actigraphy data indicated habitual good sleep (slept >6.5 h per night; slept no later than 1:00 am; woke no later than 9:00 am) for the week prior to each fMRI scanning session were included. All the participants indicated that they did not consume any medication, stimulants, caffeine, or alcohol and did not smoke for at least 24 h prior to and during each experimental session.

Study procedure

Each participant visited the laboratory for three sessions: 1) briefing, 2) rested wakefulness (RW), and 3) sleep deprivation (SD). During the briefing session, the participants were given an actigraph and issued sleep diaries. Participants were scanned during the second and third sessions, with the order of these sessions (RW and SD) counterbalanced across participants. To ensure that regular sleep times were maintained, the first scanning session followed the briefing session by at least one week. The two scan sessions were also separated by one week to minimize residual effects of SD on cognitive performance.

The participants completed a temporal discounting task (~1 hour duration) in the scanner before starting the sustained attention task. This first task presumably taxed different neural circuitry from the task of interest (Hung et al., 2013), and its effects were further reduced by giving the participants a ~15 minute break outside the scanner between tasks. The sustained attention task began at ~9:00 am (RW) or ~7:00 am (SD), times that reflect the start of a typical workday and vigilance's nadir after a night of SD, respectively (Doran et al., 2001; Graw et al., 2004). For the SD session, participants arrived by 7:00 pm and were under the constant supervision of a research assistant. Participants engaged in non-strenuous activities such as reading and watching movies, save an hourly assessment of vigilance with a 10-minute Psychomotor Vigilance Task (PVT) (Dinges et al., 1997).

Behavioral paradigm

Stimuli were generated and presented using the Psychophysics Toolbox (Brainard, 1997; Pelli, 1997) for MATLAB (2009a, 7.8.0.347; Mathworks; Natick, MA, USA). Participants viewed the stimuli through VisualSystem goggles (NordicNeuroLab; Bergen, Norway). The system's eyetracker was used to ensure that participants were awake and viewing the stimuli throughout the experiment.

While being scanned, participants completed a highly attention-demanding search task (Fig. 1) (Marois et al., 2000), designed to elicit time-on-task declines even across the task breaks (both within-run and between-run) required for BOLD fMRI. Participants attended to a rapid serial visual presentation (RSVP) stream of white letters (200 ms per item, 0.5° of visual angle; the distractor set included all non-target letters save vowels, Q, X, and Y) on a gray background, searching for the target letters J or K (inter-target interval = 2–10 s, uniform distribution). Participants identified each target as quickly as possible by pressing the response box with their right index (J) or middle (K) finger. Unlike in the PVT (Dinges et al., 1997; Lim et al., 2010b), where each target remains on screen until the subject's response, the target was presented for 200 ms and then masked by the trailing distractor regardless of reaction time. As such, this paradigm's critical behavioral measure was accuracy (Ong et al., in press; Warm et al., 2008), and visual stimulation was independent of subject performance. During each of four 6.5 minute fMRI runs, the RSVP task was presented in six task blocks (each 32 s) with fixation blocks preceding, following, and interleaved (each 24 s). Concurrent with the RSVP stream, a contrast-inversing checkerboard (10 Hz) was presented in the periphery. The luminance of the display was ~30% for half of the task blocks, but this contrast manipulation did not interact with any of our variables of interest and is not further discussed here.

Before entering the scanner, subjects practiced two blocks of the main task. Between each run, subjects rated their subjective sleepiness using the Karolinska Sleepiness Scale (KSS) (Åkerstedt and Gillberg, 1990). KSS data for one subject were not properly recorded and thus excluded.

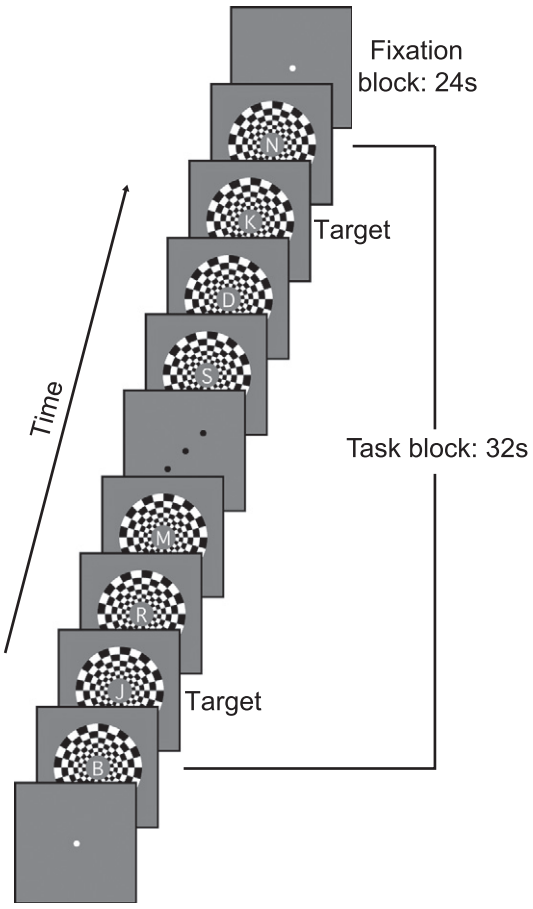

Fig. 1. Task design. Participants searched for a target letter (J or K) in a rapid serial visual presentation (RSVP) stream of distractor letters. Each frame was presented for 200 ms.

Image acquisition

Brain images were acquired on a 3 T Siemens Tim Trio (Siemens, Erlangen, Germany) at the Cognitive Neuroscience Laboratory using a 12-channel head coil. A pulsed arterial spin labeling (pASL) sequence allowed us to examine both BOLD and CBF effects. Details of this gradient echo, PICORE-Q2TIPS sequence follow: 90 volumes, TR = 4000 ms, TE = 19 ms, 90° flip angle, TI_1 = 600 ms, TI_2 = 1800 ms, 10 cm tagging region, 220 × 220 mm field of view, and a 64 × 64 matrix (in-plane resolution of 3.44 mm^2). The 22 oblique slices were each 4 mm thick (1 mm gap), oriented parallel to the AC–PC plane, positioned to capture the superior aspects of the brain, and collected in ascending sequential order. High-resolution 3D anatomical images were acquired during the evening, and T1-weighted co-planar images were acquired during each session for image co-registration.

Each scan session included four 6.5-minute task runs. Preceding and following these runs were 6.5-minute baseline CBF runs with the same scan parameters, for which subjects were instructed to keep their eyes open and fixated on a dot at the center of the gray screen. Two M_0 images were acquired at the end of each session with the same pASL parameters as before, save TR = 15000 ms. These images were used to estimate M_{0B} from M_{0WM} for the computation of quantitative CBF values (Çavuşoğlu et al., 2009; Wong et al., 1997).

Image analysis

Imaging analysis was performed using BrainVoyager QX (versions 2.4.1.2052 and 1.10.4.1250; Brain Innovation, Maastricht) and custom MATLAB software. After manual inspection for artifacts, the data were preprocessed using: 1) rigid-body motion correction (linear detection, sinc interpolation), 2) linear trend removal, and 3) spatial smoothing (8 mm FWHM Gaussian kernel). Automatic co-registration of the anatomical and functional images was checked and adjusted manually. The images were then transformed into Talairach space using an 8-point landmark approach with a piece-wise non-linear transformation.

Before submitting the data to random-effects GLM (general linear model) analysis, the timecourse of each voxel was normalized through a percent signal transformation. Separate predictors were created for the different states (RW, SD), measurement types (BOLD, CBF), runs (1–4), and blocks (1–6). These last two factors allowed us to examine between-run and within-run time-on-task effects. BOLD and CBF were modeled concurrently using the set of predictors suggested by Mumford et al. (2006). BOLD activation predictors were constructed by convolving a boxcar of hypothesized neural activity with a canonical hemodynamic response function. CBF predictors for task-related activation were constructed by multiplying the BOLD activation predictor with a predictor for baseline ASL signal (Mumford et al., 2006). Baseline CBF predictors were also constructed for the baseline runs. Finally, the GLM was fitted, correcting for serial correlations with a first-order autoregressive model.

For CBF quantification, we first reversed the percent signal change transformation by multiplying each voxel's beta weights by its average signal. The resulting values were converted to perfusion units (mL/min/100 g tissue) using the standard kinetic model (Buxton et al., 1998; Çavuşoğlu et al., 2009; Wong et al., 1998) employing the values and M_{0WM} approach described by Çavuşoğlu et al. (2009). After the CBF perfusion values were checked for reasonableness (Fig. 3) (Deibler et al., 2008), they were used for subsequent whole-brain and ROI analyses.

Activation maps were created to visualize the main effects of task, state, run, and block, and their interactions. Separate sets of maps were created for the BOLD task runs, CBF tasks runs, and CBF baseline runs. BOLD task activity was identified by comparing the estimated betas against an implicit 0-baseline (one-sample t-tests), whereas CBF task activity was defined as: (CBF task activity + CBF baseline during task runs) > (CBF during baseline runs). Between-run time-on-task effects were examined using a linear contrast across the runs ([−3/4 −1/4 1/4 3/4]); within-run time-on-task effects used the contrast ([−5/9 −3/9 −1/9 1/9 3/9 5/9]) across blocks. All maps were thresholded at $p < 0.01$, with a cluster-level threshold of $p < 0.05$ (Friston et al., 1994). This threshold is different from that typically used for BOLD imaging (Chee and Chuah, 2007; Chee et al., 2010, 2011; Kong et al., 2011, 2012; Lim et al., 2010a), and was chosen due to the lower significance values and lower spatial resolution of ASL. It closely matches the thresholds used in other ASL studies (Demeter et al., 2011; Kim et al., 2006; Lim et al., 2010b; Poudel et al., 2012).

To probe the effects of sleep deprivation and time-on-task within task-activated areas, we used the sensitive region of interest (ROI) approach. Separate CBF-based and BOLD-based sets of ROIs were defined from maps of *task activation*, as the exclusive use of either set of ROIs would be biased towards the modality from which it was defined. Additionally, the use of task-based ROIs to probe for effects of sleep deprivation and time-on-task avoids circular ROI selection (Vul et al., 2009). Each ROI was defined as the peak voxel in an anatomical region, plus all significantly activated voxels in a surrounding cube with 10 mm edges. For ROI analyses, the beta weights from the ROI voxels were averaged and then compared across conditions using t-tests, with effect sizes assessed using η^2.

Results

Subjective sleepiness

A two-way, repeated-measures ANOVA assessed the effects of state and time-on-task (between-run) on subjective sleepiness reports from

19 of 20 subjects (see Section Behavioral paradigm). Sleepiness was greater during the SD session ($F_{1,18} = 75$, $p < 0.0001$) and differed by run ($F_{4,72} = 4.5$, $p < 0.01$), increasing over the course of each session (linear contrast: $t_{18} = 4.3$, $p < 0.001$). State and time-on-task did not significantly interact ($F_{4,72} = 0.59$, n.s.; linear interaction contrast: $t_{18} = 0.49$, n.s.).

Behavioral findings

The task proved demanding, and subject performance was affected by both state (SD versus RW) and time-on-task (ToT) (Fig. 2). A two-way, repeated-measures ANOVA on target detection rate found main effects of state ($F_{1,19} = 24$, $p < 0.0001$) and run ($F_{3,57} = 2.9$, $p < 0.05$), with performance marginally declining across time (linear contrast for between-run ToT: $t_{19} = 2.0$, $p = 0.062$). State and run also showed a marginal interaction ($F_{3,57} = 2.6$, $p = 0.058$), though between-run ToT effects were not significantly different across state (linear interaction contrast: $t_{19} = 1.4$, n.s.). As the number of targets per block was low (5.3 on average), we pooled block performance across runs and used a separate ANOVA to investigate within-run ToT effects and their interaction with state. (A comparable procedure was used when analyzing false alarms and reaction times.) This test revealed a main effect of block ($F_{5,95} = 3.1$, $p < 0.01$), with target detection declining within runs (linear contrast for within-run ToT: $t_{19} = 2.9$, $p < 0.01$). Although the interaction of state and block did not reach significance ($F_{5,95} = 1.8$, $p = 0.12$), a linear interaction contrast suggested that the ToT decline was greater during SD ($t_{19} = 4.0$, $p < 0.001$).

The decrease in accuracy during SD was accompanied by more false alarms (Supp. Figs. 1A–C). Two-way, repeated measures ANOVAs on false alarms (after removal of an outlier subject, who had 125 false alarms in SD and 13 in RW) confirmed this significant state effect ($F_{1,18} = 7.7$, $p < 0.05$), but there were no significant changes in false alarms across time, either between-run (run: $F_{3,54} = 0.38$, n.s.) or within-run (block: $F_{5,90} = 1.1$, n.s.). State and ToT also did not interact (state × run: $F_{3,54} = 0.33$, n.s.; state × block: $F_{5,90} = 0.70$, n.s.). These results indicate that participants still attempted to perform the task even when fatigued.

Before testing for reaction time effects, we calculated each subject's median reaction time for each condition combination (state × block or state × run). Reaction times were longer in SD, but they were not significantly affected by ToT (Supp. Figs. 1D–F). Two-way, repeated-measures ANOVAs on reaction time found main effects of state ($F_{1,19} = 11$, $p < 0.01$), but no ToT effects (run: $F_{3,57} = 1.1$, n.s.; block: $F_{5,95} = 1.7$, n.s.). State and ToT did not interact (state × run: $F_{3,57} = 0.13$, n.s.; state × block: $F_{5,95} = 0.75$, n.s.). Coupled with the declines in accuracy related to both SD and ToT, the reaction time results demonstrate the absence of a large change in the speed-accuracy trade-off across state and time.

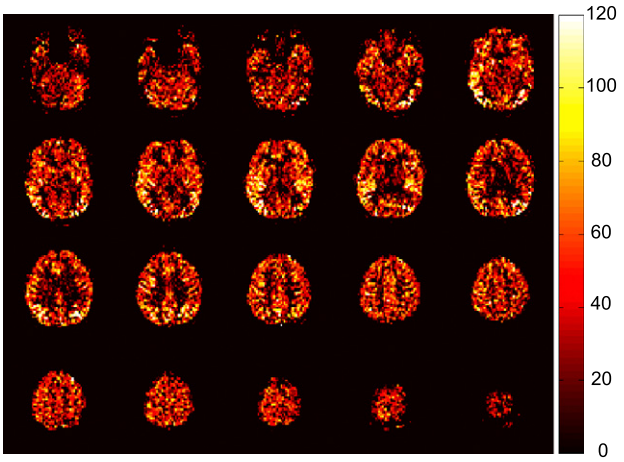

Fig. 3. Quantitative CBF maps from a representative subject. Units are mL/min/100 g tissue.

Imaging

The average whole-brain CBF value collapsed across the resting baseline conditions was 44.9 +/− 5.6 mL/min/100 g tissue (mean +/− standard deviation). A two-way, repeated-measures ANOVA found neither effects of state ($F_{3,57} = 0.81$, n.s.) nor time-on-task ($F_{3,57} = 0.36$, n.s.) on these whole-brain measures of resting baseline CBF. For both whole-brain and regional analyses of resting baseline CBF, we assessed state effects by contrasting the pre- and post-task RW resting baseline runs with the corresponding runs in SD, and we assessed ToT effects by contrasting the RW and SD pre-task resting baseline runs with the corresponding post-task runs. The whole-brain resting baseline CBF values are lower than what is often reported for ASL studies (Lim et al., 2010b), but this discrepancy can be explained by our use of a Q2TIPS sequence (~18% lower calculated CBF than FAIR-QII) and white matter-based CBF estimation (~16% lower calculated CBF than with quantification based on M_{0T}). (Çavuşoğlu et al., 2009).

Below we present the results for each comparison (task, state, time-on-task) separately, detailing the BOLD effects, CBF effects (task-evoked signal), and CBF resting baseline changes for each effect type. No significant interactions were found among the conditions, so only main effects are discussed. In addition, no significant activation increases were found for state (SD > RW) or time-on-task (greater activation across successive runs or blocks). For display purposes,

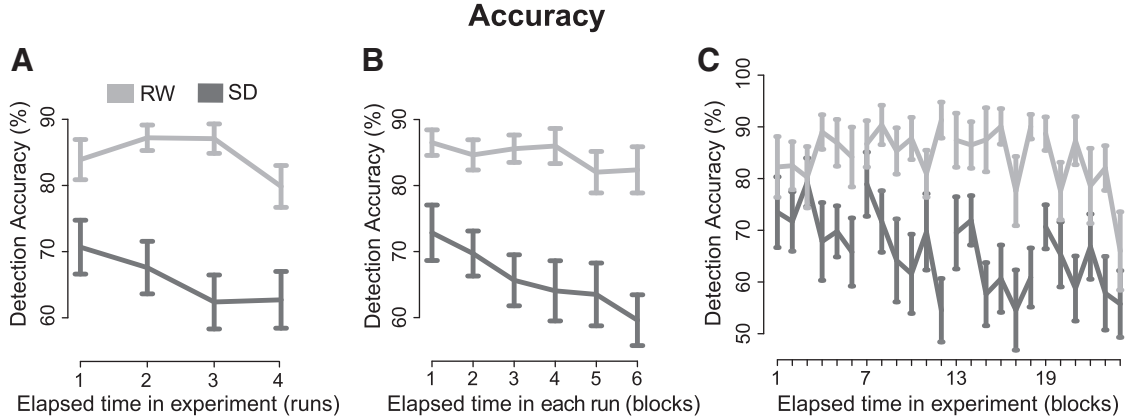

Fig. 2. Effects of state and time-on-task on target detection rate. (A) Performance by run in each state. (B) Performance by block in each state, averaged across runs. (C) Performance by block across the entire experiment. Error bars are standard error of the mean.

Table 1
Effect sizes (η^2) for BOLD task-related, CBF task-related, and CBF resting baseline effects for task, state, and time-on-task (ToT) in BOLD-defined ROIs.

Region	Hemi	BA	Tal	Task		State			ToT (between)			ToT (within)	
			x, y, z	BOLD	CBF	BOLD	CBF	Baseline	BOLD	CBF	Baseline	BOLD	CBF
IPS	R	7, 39	25, −57, 38	**		**	*		*		**	**	
	L		−28, −58, 38	***	*	**			**			**	
MFG	R	6, 9	38, −1, 30	***	*	*			**			*	
	L		−44, 1, 29	***	**	**		*	**	**		***	
SMFC	R	6, 32	3, 8, 48	***		*			***			***	
	L		−7, 4, 47	***					**			***	
AI	R	13	34, 13, 7	***	*				**			***	
	L		−33, 17, 7	***					**			***	
VVC	R	19, 37	35, −71, −6	***	***	**	**		**	***	**	**	
	L		−43, −67, −5	***	***	**	**		**	*	**	**	
EVC	R	17, 18	2, −84, −7	***	**		*			**		***	
	L		−7, −83, −8	***	***		**	(**)		**		***	
Thal	R		11, −8, 7	***					**	*		***	
	L		−19, −4, 10	***					***			**	

Number of asterisks indicates the effect size. * represents $\eta^2 > 0.14$ (marginal effect for paired samples t-test, $p < 0.10$), ** represents $\eta^2 > 0.19$ ($p < 0.05$), and *** represents $\eta^2 > 0.44$ ($p < 0.001$). Comparisons for task-related activity are Task: (Task–Baseline; see Materials and methods), State: (SD–RW), ToT (between): linear contrast [−3/4 −1/4 1/4 3/4], and ToT (within): linear contrast [−5/9 −3/9 −1/9 1/9 3/9 5/9]. For Baseline, the comparisons are State: ((pre-task SD + post-task SD)–(pre-task RW + post-task RW)) and ToT (between): ((post-task SD + post-task RW)–(pre-task SD + pre-task RW)). RW = rested wakefulness, SD = sleep deprivation. Note that all state and time-on-task effects represented declines in activation except where indicated with parentheses. BA = Brodmann Area, Tal = Talairach coordinates (Talairach and Tournoux, 1988), IPS = intra-parietal sulcus, MFG = middle frontal gyrus, SMFC = superior medial frontal cortex, AI = anterior insula, VVC = ventral visual cortex, EVC = early visual cortex, Thal = thalamus.

ROI activations are plotted collapsed across hemispheres; tables provide these values for ROIs split by hemisphere.

Imaging: task effects

The task elicited significant BOLD signal changes in the intra-parietal sulcus (IPS), middle frontal gyrus (MFG), superior medial frontal cortex, anterior insula, ventral visual cortex, early visual cortex and the thalamus (Table 1; Inline Supplementary Table S1; Figs. 4A, B). All structures were activated bilaterally.

Inline Supplementary Table S1 can be found online at http://dx.doi.org/10.1016/j.neuroimage.2013.05.119.

ASL revealed areas congruent with those found with BOLD imaging, but these were fewer in number. Task-evoked activity was found in left MFG, left insula, right frontal pole, bilateral ventral visual cortex, bilateral early visual cortex, and bilateral thalamus (Fig. 4A). ROI analyses showed that CBF effects were weaker than corresponding BOLD ones (Table 1). BOLD effects were generally stronger even within CBF-defined ROIs. Furthermore, because BOLD-defined and CBF-defined ROIs yielded comparable results for both task-related activity and higher-order comparisons (Inline Supplementary Table S2), we focus on the more numerous BOLD-defined ROIs henceforth.

Inline Supplementary Table S2 can be found online at http://dx.doi.org/10.1016/j.neuroimage.2013.05.119.

Imaging: state

State differences in BOLD signal were observed in many regions recruited during the task (Fig. 4D). Bilateral fronto-parietal cortices and ventral visual cortex showed significant declines in BOLD signal during SD (Fig. 4B). Notably absent were early visual regions. The ROI analysis confirmed this difference, with both thalamic and early visual areas showing no consistent modulation by state (Table 1).

State effects assessed using ASL found significant declines in ventral visual cortex, but effects in the fronto-parietal cortices failed to reach significance (Table 1; Fig. 4C). Unlike the BOLD imaging findings, task-evoked CBF in left early visual cortex also declined in SD. This decline in task-evoked signal, however, was accompanied by a significant *increase* in CBF across the resting baseline runs (pre-task + post-task in RW versus pre-task + post-task in SD) in early visual cortex, making the findings difficult to interpret (Inline Supplementary Table S1). Early visual cortex was the only region to show such an increase. Otherwise, SD-related changes to resting baseline CBF were primarily non-significant declines (Fig. 7A).

Imaging: time-on-task (between-run)

Similar to the state effects, time-on-task effects with BOLD fMRI were observed in many task-activated regions (Fig. 5A), including the same fronto-parietal and ventral visual areas that showed state effects. In addition, ToT effects were found in the thalamus, insula, and medial frontal cortex, most clearly revealed in the ROI analyses (Table 1; Fig. 5B). In contrast, early visual cortex activation did not decline across runs.

ToT effects on CBF were weakly congruent with the BOLD findings. Declines in task-related CBF were evidenced in left MFG and in ventral visual cortex. In contrast to the BOLD results, however, the early visual areas showed decreased CBF as the task progressed. Finally, resting baseline CBF was little affected by having performed the task (Table 1). Two exceptions were the ventral visual cortex and right IPS, which showed lower baseline CBF after the task (Fig. 7B).

Imaging: time-on-task (within-run)

Within-run time-on-task effects on BOLD signal were congruent with the between-run ToT effects (Fig. 6A). All probed task-activated regions showed declines across time (Table 1; Fig. 6B). In contrast, CBF measures of within-run ToT effects showed high variance with no significant effects.

Imaging: BOLD functional overlap

To visualize the degree of functional overlap across the BOLD activation maps, we overlayed the task, state, and time-on-task results (Fig. 8). These maps show triple overlaps in the middle frontal gyrus (MFG) and ventral visual cortex. As such, they are consistent with the region-of-interest analyses, which found significant task, state, and time-on-task results in both of these regions and also the intra-parietal sulcus (IPS; Table 1). In addition, the two measures of time-on-task, within-run and between-run, showed considerable functional overlap (Supp. Fig. 2; Table 1).

Discussion

In the current study, we compared the effects of sleep deprivation and time-on-task within the brain areas recruited during an attentionally-demanding task. Our comparisons included task-related BOLD and ASL signal changes across both rested and sleep deprived conditions. We also examined ASL signal in the absence of task performance to examine changes in baseline CBF. The long scan sessions (26 min of task, 13 min of

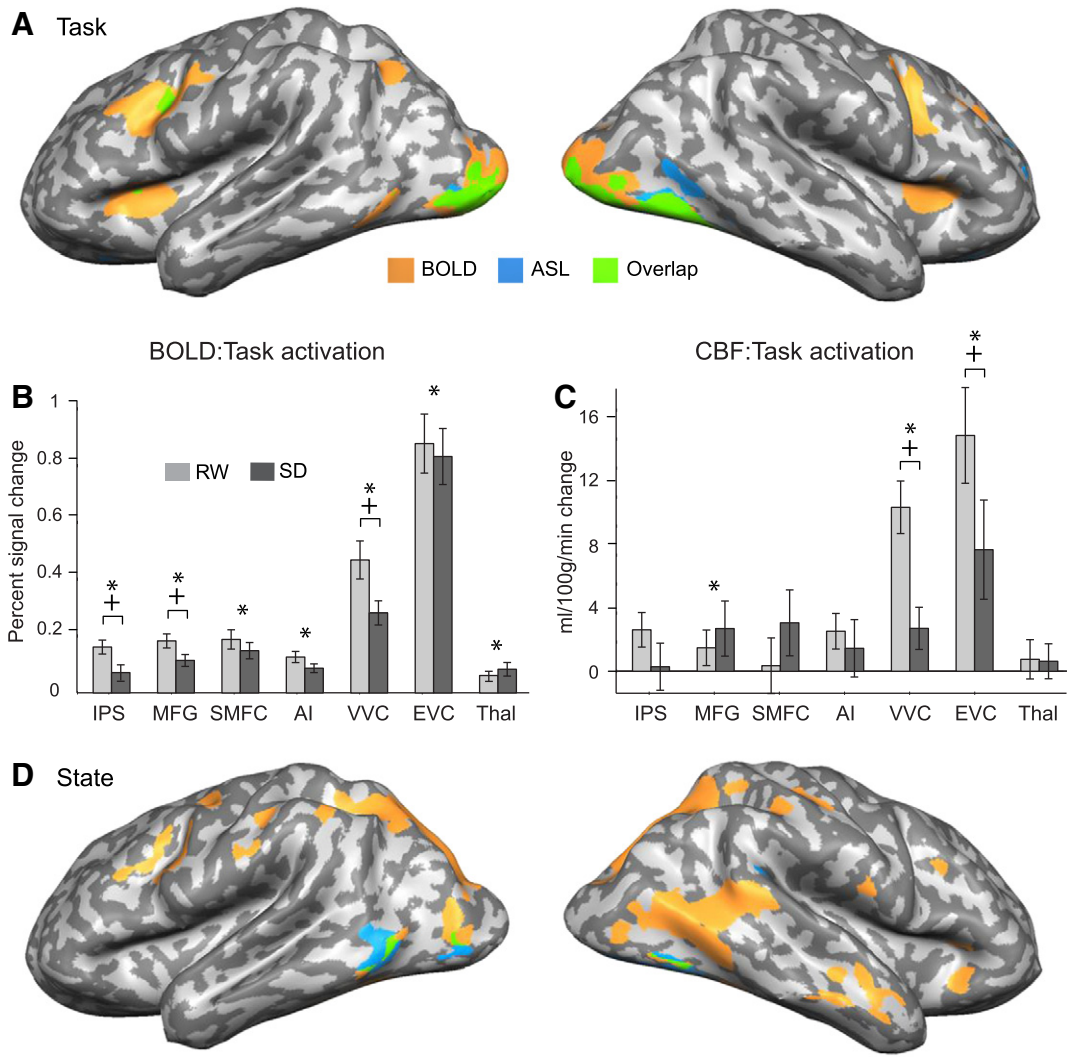

Fig. 4. Task activations and state effects. (A) Regions recruited by the target detection task, as reflected in BOLD or CBF changes. All maps shown with nominal threshold of $p < 0.01$, cluster-corrected to $p < 0.05$. (B) BOLD task activation in select regions of interest (ROIs) collapsed across hemispheres. Asterisks indicate significant main effects of task ($p < 0.05$), whereas pluses indicate significant state effects ($p < 0.05$). Error bars are SEM. (C) CBF task activation in select ROIs. (D) Regions with significantly greater activation during rested wakefulness compared to following sleep deprivation. IPS = intra-parietal sulcus, MFG = middle frontal gyrus, SMFC = superior medial frontal cortex, AI = anterior insula, VVC = ventral visual cortex, EVC = early visual cortex.

task-free baseline) allowed us to examine time-on-task effects, SD effects, and baseline shifts with considerably more power than previous studies (Lim et al., 2010b; Poudel et al., 2012).

Consistent with earlier work (Van Dongen et al., 2011; Warm et al., 2008; Wilkinson, 1964), we found that sleep deprivation exacerbated time-on-task effects. Examination of task-activated regions of interest found partially congruent reductions of BOLD signal for SD and time-on-task effects, particularly in the ventral visual cortex and fronto-parietal attention regions. In regions where the effect sizes were sufficiently large to observe SD and time-on-task effects on CBF, particularly ventral visual cortex, the CBF changes were consistent with the BOLD measures. Furthermore, resting baseline CBF was largely unchanged across state or after task performance. Taken together, these results suggest that BOLD findings are likely uncontaminated by altered coupling with or baseline shifts in CBF.

Concurrence of BOLD and CBF measures of task-related brain activation

Our results show a general agreement between BOLD and CBF. Both measures identified task activation in ventral visual cortex and fronto-parietal attention regions. Both measures also identified declines in ventral visual cortex with time-on-task and sleep deprivation. Although BOLD revealed additional declines in fronto-parietal cortex, this finding was likely due to this technique's greater signal-to-noise ratio (Parrish et al., 2000). Indeed, the observed BOLD measurements had consistently higher statistical significance values than their CBF counterparts (Table 1; Inline Supplementary Table S2).

Although BOLD affords a higher signal-to-noise ratio as well as the possibility of collecting more images per unit time with better spatial resolution, ASL has the advantage of long-term signal stability (Demeter et al., 2011; Lim et al., 2010b; Rao, 2012). This property makes ASL well suited for studying gradual shifts in neural activity (Aguirre et al., 2002; Wang et al., 2005), such as those expected across runs in the current task. Indeed, our CBF results show clearer ToT effects between runs than within them, whereas the BOLD results show the reverse. This pattern of results highlights ASL's relative advantage in making comparisons across longer time intervals. Nevertheless, BOLD fMRI's superior signal-to-noise ratio was a more important factor here, as BOLD effect sizes were greater than ASL's for both between- and within-run ToT effects.

Biophysical models of BOLD suggest that its signal changes are a function of CBF, cerebral blood volume, and cerebral oxygen metabolic rate (Ances et al., 2009; Davis et al., 1998; Kim et al., 1999; Mandeville

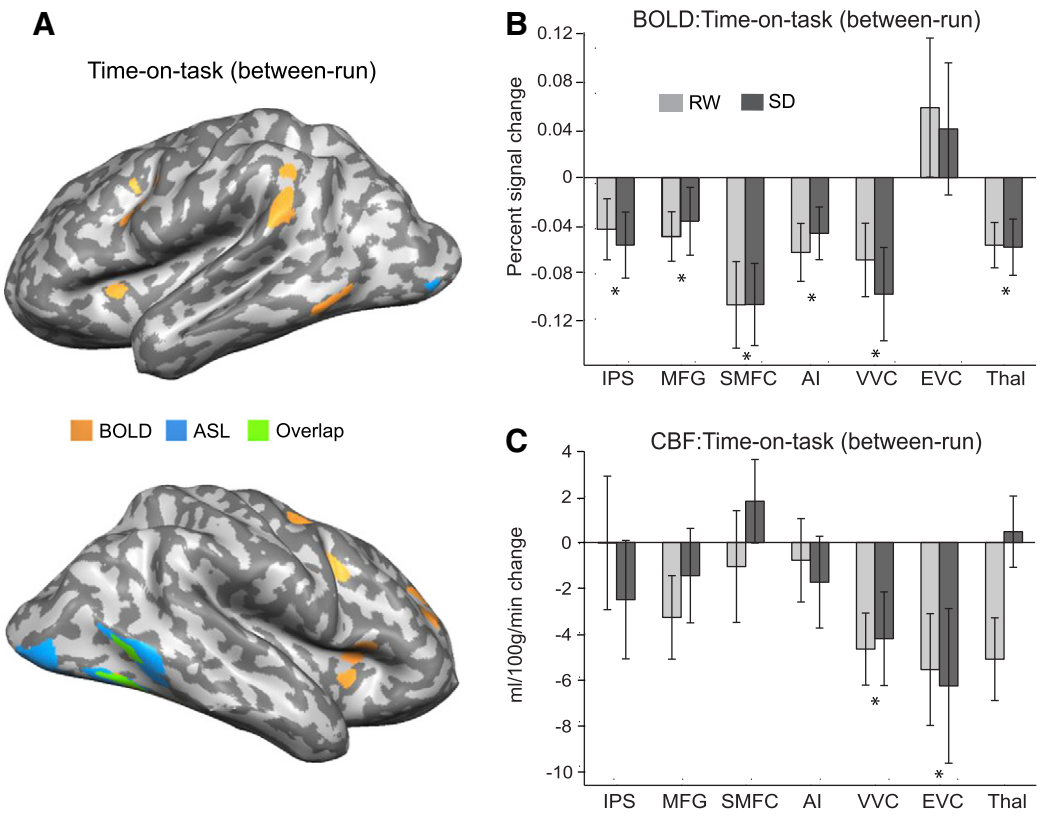

Fig. 5. Time-on-task effects, across-run. (A) Regions with significant declines in activation across the four task runs (collapsed across state). (B) BOLD time-on-task effects in select regions of interest (ROIs). Effects were calculated with the linear contrast [−3/4 −1/4 1/4 3/4], as there were four task runs. Asterisks indicate significant main effects of time-on-task ($p < 0.05$). (C) CBF time-on-task effects in select ROIs.

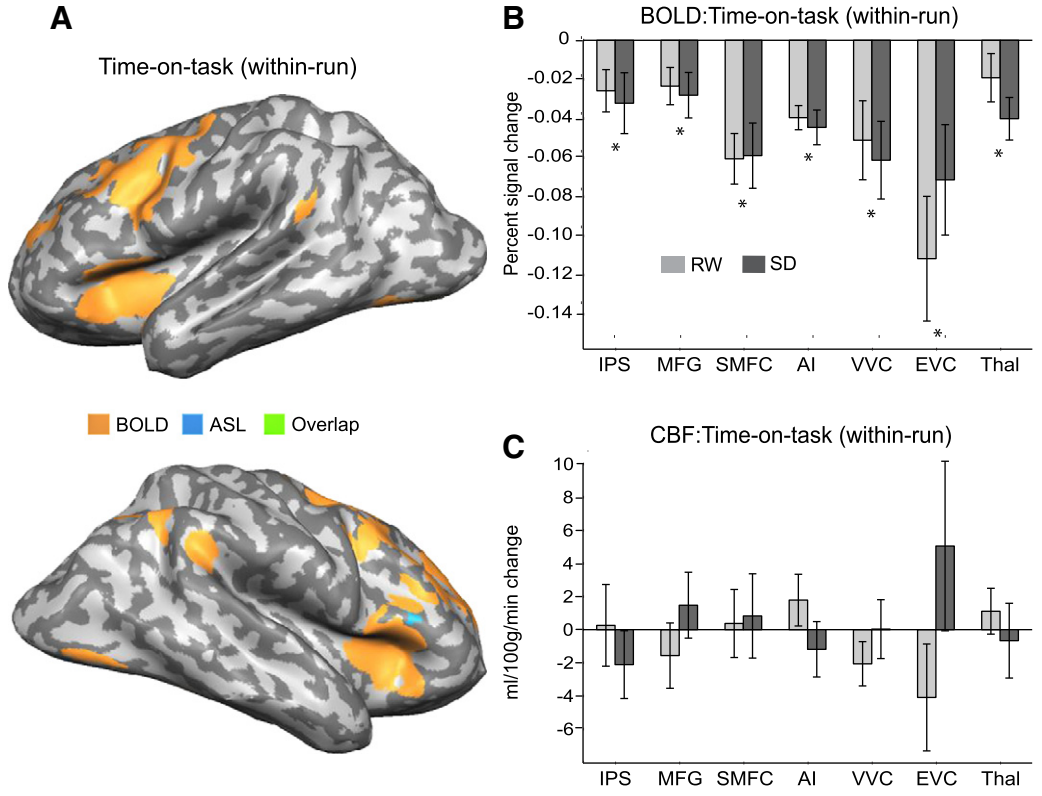

Fig. 6. Time-on-task effects, within-run. (A) Regions with significant declines in activation during each task run (collapsed across state). (B) BOLD time-on-task effects in select regions of interest (ROIs). Effects were calculated with the linear contrast [−5/9 −3/9 −1/9 1/9 3/9 5/9], as there were six blocks within each run. Asterisks indicate significant main effects of time-on-task ($p < 0.05$). (C) CBF time-on-task effects in select ROIs.

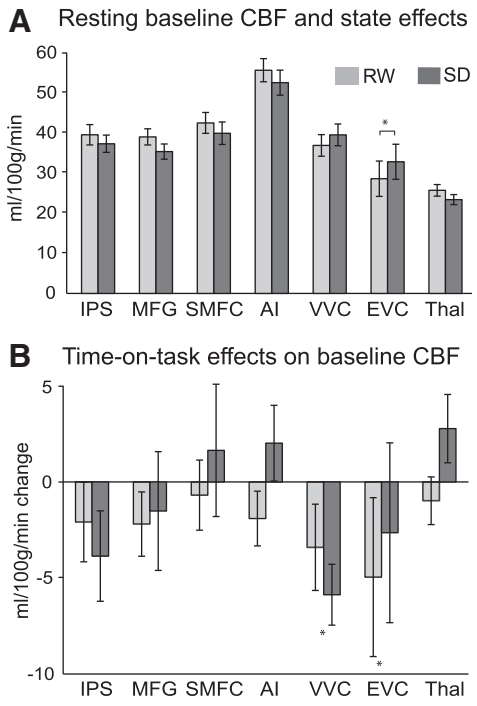

Fig. 7. Baseline CBF in regions of interest. (A) Baseline CBF values across state. Asterisks indicate significant state effects. (B) Effects of time-on-task on baseline CBF. Asterisks indicate significant time-on-task effects.

et al., 1999; Rao, 2012; Shen et al., 2008). Despite the BOLD signal's sensitivity to these different physiological changes, the similar inferences drawn from BOLD and CBF results suggests that neither sleep deprivation nor time-on-task significantly decouples these two measures. Previous research in elderly subjects had found such decoupling, suggesting that vascular changes (perhaps those reflected in baseline CBF changes) may alter the BOLD signal (Ances et al., 2009; Bangen et al., 2009). These resting baseline CBF changes in the elderly were typically on the order of 30–40%, far larger than any of the baseline effects we observed.

Convergence of sleep deprivation and time-on-task effects

Behavioral studies of vigilant attention show that sleep deprivation and time-on-task interact to decrease performance (Van Dongen et al., 2011; Warm et al., 2008; Wilkinson, 1964). This interaction suggests that similar processing stages (Schweickert, 1985; Sternberg, 1969) and, perhaps, similar brain regions may underlie such declines, with the most likely candidates being regions in the frontal and parietal cortices involved in the top-down control of attention (Corbetta and Shulman, 2002; Kastner et al., 1999). Indeed, frontal and parietal regions show activation declines in a broad array of sleep deprivation (Chee and Chuah, 2007, 2008; Chee et al., 2010; Kong et al., 2011, 2012; Lim et al., 2010a) and time-on-task studies (Coull et al., 1998; Lim et al., 2010b). Here, we compared the neural correlates of these effects directly, and found that the sleep deprivation and time-on-task affected an overlapping subset of the task-activated regions, including frontal-parietal attention regions and ventral visual cortex (Fig. 8).

These imaging findings prompt a question: Why were many of the regions mediating attention affected by both sleep deprivation and time-on-task? One possibility is that attentional circuits become fatigued with repeated use (Krueger and Obál, 1993; Van Dongen et al., 2011). This use-dependency account suggests that either prolonged wake or sustained task engagement exhausts the neural circuits supporting attention (Hung et al., 2013). Resource theories of ToT are consistent with this account, as they argue that sustained attention requires effort and therefore drains cognitive resources (Smit et al., 2004; Warm et al., 2008). These same resources are thought to be limited during sleep deprivation (Kong et al., 2011, 2012), leading to more severe ToT effects in that state.

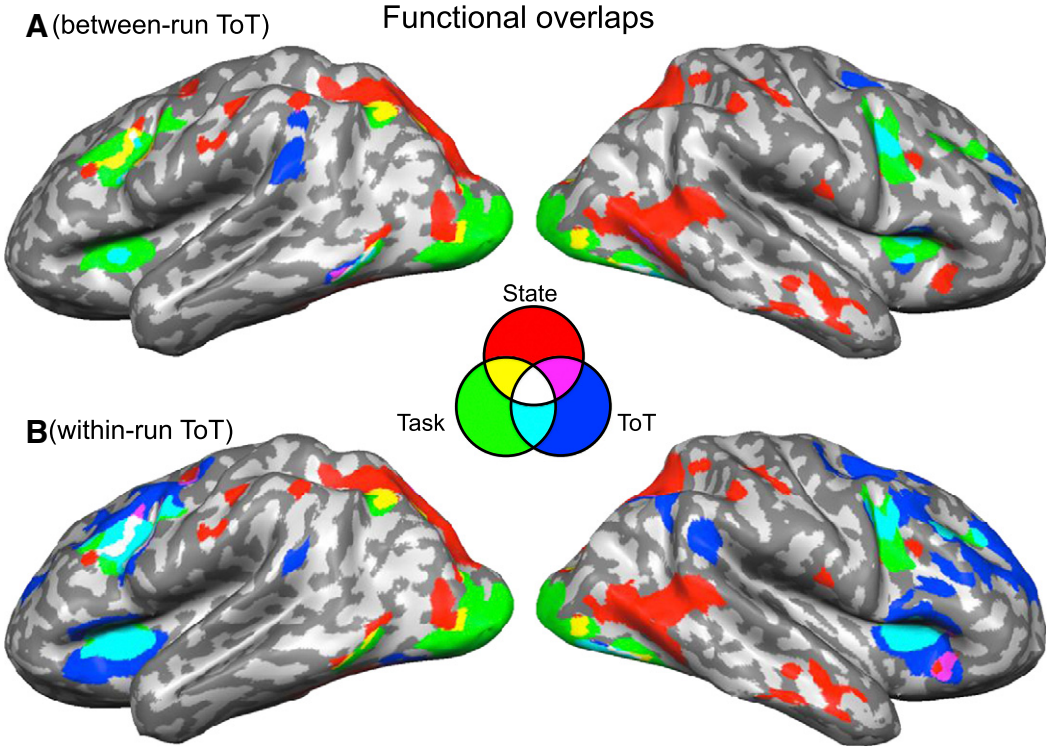

Fig. 8. Overlap of BOLD activation associated with task, state, and time-on-task. (A) Overlaps for between-run time-on-task. (B) Overlaps for within-run time-on-task. Note the three-way overlap of activation in the middle frontal gyrus and ventral visual cortex.

An alternative possibility is that sleep deprivation and time-on-task both impair participant motivation, thereby leading to poorer performance and reduced activity (Lim et al., 2010b; Mackworth, 1968). In the present experiment, however, participants continued to put effort into the task, as evidenced by increasing false alarms as the target detection rates dropped. Such results suggest a shift in detection ability, not failure to engage with the task (Langner et al., 2010).

In addition to neural convergence of SD and ToT effects, our results include a number of dissociations. Particularly for our CBF results, some regions may have failed to show ToT effects owing to the breaks (both within-run and between-run) needed for BOLD fMRI (Ong et al., in press) or subjects' recent completion of an hour-long temporal discounting task—both despite the presence of behavioral ToT effects. Other differences, however, may reflect partially dissociable cognitive processes. One potential explanation for such differences is that SD and ToT affect the ability to perform and motivation to different degrees. Alternatively, ToT effects, unlike SD ones, may reflect a shift from controlled to automatic processing (Coull et al., 1998; Paus et al., 1997). We find such an explanation for our results unsatisfactory, however, for unlike the oddball paradigms employed in many other sustained attention studies, our task required a continuous and effortful search. It is unlikely that performance could have been largely preserved if participants switched to an automatic strategy of target detection (Lim et al., 2010b).

Changes in regional CBF at rest

In the present study, only early visual cortex showed resting baseline CBF changes due to sleep deprivation. Extant studies have offered conflicting results of such baseline effects. For example, overall decreases (Thomas et al., 2000; Wu et al., 2006), increases (Braun et al., 1997), or lack of change (Poudel et al., 2012; Wu et al., 1991) in baseline activity have been reported during SD. Regional differences have shown similar inconsistency. For example, visual cortex effects have ranged from no change (Poudel et al., 2012; Thomas et al., 2000; Wu et al., 1991) to *increases* during SD (Braun et al., 1997; Wu et al., 2006). Numerous factors may account for these differences. First, many studies include a behavioral task (e.g. continuous performance task or serial addition/subtraction) during their baseline scans (Thomas et al., 2000; Wu et al., 1991; Wu et al., 2006). As such, their reported CBF changes may include both task-evoked signal and baseline shifts. Second, some studies compared CBF during sleep deprivation to CBF immediately after recovery sleep (Braun et al., 1997; Wu et al., 2006). Third, a recent study reported large individual differences in CBF based on participants' drowsiness (Poudel et al., 2012). Our study attempted to minimize these factors (with the exception of sleepiness), and found that resting baseline CBF was largely unchanged by state.

Similarly, few regions in the current study showed baseline CBF declines after extended task performance. Only ventral visual cortex and right IPS showed such declines, possibly due to their heavy engagement during the task. These results and their explanation are consistent with previous studies of ToT (Lim et al., 2010b). In addition, the detection of such changes implies that our study had the power to reveal baseline CBF changes, but SD did not induce consistent baseline shifts (save in early visual cortex).

Coupled with the observed state and ToT imaging effects, the paucity of resting baseline changes in the current study suggests that many effects of state are only apparent during task performance itself, not in any regional changes to resting baseline CBF. For example, in the current study, regions mediating attention showed evoked BOLD and CBF signal differences only during the attention-demanding task; in contrast, they showed no resting baseline differences as either a function of state or ToT. To the extent that this result generalizes, it suggests that other latent deficits—or spared function—may be uncovered by employing different tasks.

Conclusion

The present study adds evidence to the suggestion that the deleterious effects of sleep deprivation and time-on-task on sustained attention have shared neural and psychological causes. The results also suggest that BOLD fMRI studies reflect changes in task-related neural activation in sleep deprived persons. Our BOLD and CBF measures resulted in compatible inferences about the effects of SD. There were few substantial baseline shifts in CBF across conditions. The paucity of such baseline shifts indicates that the neural consequences of sleep deprivation are apparent primarily in the evoked signals within task-relevant brain regions. Given our findings and the generally better SNR of BOLD, we suggest that BOLD fMRI be used for the majority of sleep deprivation studies.

Supplementary data to this article can be found online at http://dx.doi.org/10.1016/j.neuroimage.2013.05.119.

Acknowledgments

The authors thank Xavier Golay and Wen-Chau Wu for technical assistance and helpful discussion. They also thank Joann Poh, Deepti Mulick, and Jack De Havas Gwenlan for help with data processing and manuscript preparation.

Conflict of interest statement

The authors certify that they have no conflicts of interest.

References

Aguirre, G.K., Detre, J.A., Zarahn, E., Alsop, D.C., 2002. Experimental design and the relative sensitivity of bold and perfusion fMRI. NeuroImage 15, 488–500.
Åkerstedt, T., Gillberg, M., 1990. Subjective and objective sleepiness in the active individual. Int. J. Neurosci. 52, 29–37.
Ances, B.M., Liang, C.L., Leontiev, O., Perthen, J.E., Fleisher, A.S., Lansing, A.E., Buxton, R.B., 2009. Effects of aging on cerebral blood flow, oxygen metabolism, and blood oxygenation level dependent responses to visual stimulation. Hum. Brain Mapp. 30, 1120–1132.
Bangen, K.J., Restom, K., Liu, T.T., Jak, A.J., Wierenga, C.E., Salmon, D.P., Bondi, M.W., 2009. Differential age effects on cerebral blood flow and BOLD response to encoding: associations with cognition and stroke risk. Neurobiol. Aging 30, 1276–1287.
Bell-McGinty, S., Habeck, C., Hilton, H.J., Rakitin, B., Scarmeas, N., Zarahn, E., Flynn, J., DeLaPaz, R., Basner, R., Stern, Y., 2004. Identification and differential vulnerability of a neural network in sleep deprivation. Cereb. Cortex 14, 496–502.
Brainard, D.H., 1997. The Psychophysics Toolbox. Spat. Vis. 10, 433–436.
Braun, A.R., Balkin, T.J., Wesenten, N.J., Carson, R.E., Varga, M., Baldwin, P., Selbie, S., Belenky, G., Herscovitch, P., 1997. Regional cerebral blood flow throughout the sleep-wake cycle. An H2(15)O PET study. Brain 120, 1173–1197.
Brown, G.G., Clark, C., Liu, T.T., 2007. Measurement of cerebral perfusion with arterial spin labeling: part 2. Application. J. Int. Neuropsychol. Soc. 13, 526–538.
Buxton, R.B., Frank, L.R., Wong, E.C., Siewert, B., Warach, S., Edelman, R.R., 1998. A general kinetic model for quantitative perfusion imaging with arterial spin labeling. Magn. Reson. Med. 40, 383–396.
Çavuşoğlu, M., Pfeuffer, J., Uğurbil, K., Uludağ, K., 2009. Comparison of pulsed arterial spin labeling encoding schemes and absolute perfusion quantification. Magn. Reson. Imaging 27, 1039–1045.
Chee, M.W.L., Chuah, L.Y.M., 2007. Functional neuroimaging and behavioral correlates of capacity decline in visual short-term memory after sleep deprivation. Proc. Natl. Acad. Sci. U. S. A. 104, 9487–9492.
Chee, M.W.L., Chuah, L.Y.M., 2008. Functional neuroimaging insights into how sleep and sleep deprivation affect memory and cognition. Curr. Opin. Neurol. 21, 417–423.
Chee, M.W., Tan, J.C., Parimal, S., Zagorodnov, V., 2010. Sleep deprivation and its effects on object-selective attention. NeuroImage 49, 1903–1910.
Chee, M.W.L., Goh, C.S., Namburi, P., Parimal, S., Seidl, K.N., Kastner, S., 2011. Effects of sleep deprivation on cortical activation during directed attention in the absence and presence of visual stimuli. NeuroImage 58, 595–604.
Corbetta, M., Shulman, G.L., 2002. Control of goal-directed and stimulus-driven attention in the brain. Nat. Rev. Neurosci. 3, 215–229.
Coull, J.T., Frackowiak, R.S.J., Frith, C.D., 1998. Monitoring for target objects: activation of right frontal and parietal cortices with increasing time on task. Neuropsychologia 36, 1325–1334.
Davis, T.L., Kwong, K.K., Weisskoff, R.M., Rosen, B.R., 1998. Calibrated functional MRI: mapping the dynamics of oxidative metabolism. Proc. Natl. Acad. Sci. U. S. A. 95, 1834–1839.
Deibler, A.R., Pollock, J.M., Kraft, R.A., Tan, H., Burdette, J.H., Maldjian, J.A., 2008. Arterial spin-labeling in routine clinical practice, part 1: Technique and artifacts. Am. J. Neuroradiol. 29, 1228–1234.

Demeter, E., Hernandez-Garcia, L., Sarter, M., Lustig, C., 2011. Challenges to attention: a continuous arterial spin labeling (ASL) study of the effects of distraction on sustained attention. NeuroImage 54, 1518–1529.
Dinges, D.F., Pack, F., Williams, K., Gillen, K.A., Powell, J.W., Ott, G.E., Aptowicz, C., Pack, A.I., 1997. Cumulative sleepiness, mood disturbance, and psychomotor vigilance performance decrements during a week of sleep restricted to 4-5 hours per night. Sleep 20, 267–277.
Doran, S.M., Van Dongen, H.P.A., Dinges, D.F., 2001. Sustained attention performance during sleep deprivation: evidence of state instability. Arch. Ital. Biol. 139, 253–267.
Friston, K.J., Worsley, K.J., Frackowiak, R.S.J., Mazziotta, J.C., Evans, A.C., 1994. Assessing the significance of focal activations using their spatial extent. Hum. Brain Mapp. 1, 210–220.
Grant, D.A., Rector, D.M., Van Dongen, H.P.A., Belenky, G., 2009. Prefrontal hemodynamic signals measured by near-infrared optical topography are correlated with attentional lapses on a psychomotor vigilance test. Sleep 32 (Suppl. 1), A24.
Graw, P., Krauchi, K., Knoblauch, V., Wirz-Justice, A., Cajochen, C., 2004. Circadian and wake-dependent modulation of fastest and slowest reaction times during the psychomotor vigilance task. Physiol. Behav. 80, 695–701.
Habeck, C., Rakitin, B.C., Moeller, J., Scarmeas, N., Zarahn, E., Brown, T., Stern, Y., 2004. An event-related fMRI study of the neurobehavioral impact of sleep deprivation on performance of a delayed-match-to-sample task. Brain Res. Cogn. Brain Res. 18, 306–321.
Hoge, R.D., Atkinson, J., Gill, B., Crelier, G.R., Marrett, S., Pike, G.B., 1999. Linear coupling between cerebral blood flow and oxygen consumption in activated human cortex. Proc. Natl. Acad. Sci. U. S. A. 96, 9403–9408.
Horne, J.A., Östberg, O., 1976. A self-assessment questionnaire to determine morningness-eveningness in human circadian rhythms. Int. J. Chronobiol. 4, 97–110.
Hung, C.S., Sarasso, S., Ferrarelli, F., Riedner, B., Ghilardi, M.F., Cirelli, C., Tononi, G., 2013. Local experince-dependent changes in the wake EEG after prolonged wakefulness. Sleep 36, 59–72.
Kastner, S., Pinsk, M.A., De Weerd, P., Desimone, R., Ungerleider, L.G., 1999. Increased activity in human visual cortex during directed attention in the absence of visual stimulation. Neuron 22, 751–761.
Kim, S.G., Rostrup, E., Larsson, H.B.W., Ogawa, S., Paulson, O.B., 1999. Determination of relative CMRO2 from CBF and BOLD changes: significant increases of oxygen consumption rate during visual stimulation. Magn. Reson. Med. 41, 1152–1161.
Kim, J., Whyte, J., Wang, J., Rao, H., Tang, K.Z., Detre, J.A., 2006. Continuous ASL perfusion fMRI investigation of higher cognition: quantification of tonic CBF changes during sustained attention and working memory tasks. NeuroImage 31, 376–385.
Kong, D., Soon, C.S., Chee, M.W.L., 2011. Reduced visual processing capacity in sleep deprived persons. NeuroImage 55, 629–634.
Kong, D., Soon, C.S., Chee, M.W.L., 2012. Functional imaging correlates of impaired distractor suppression following sleep deprivation. NeuroImage 61, 50–55.
Krueger, J.M., Obál, F., 1993. A neuronal group theory of sleep function. J. Sleep Res. 2, 63–69.
Langner, R., Eickhoff, S.B., 2012. Sustaining attention to simple tasks: a meta-analytic review of the neural mechanisms of vigilant attention. Psychol. Bull. (Advanced online publication). http://dx.doi.org/10.1037/a0030694, PMID: 23163491.
Langner, R., Steinborn, M.B., Chatterjee, A., Sturm, W., Willmes, K., 2010. Mental fatigue and temporal preparation in simple reaction-time performance. Acta Psychol. 133, 64–72.
Lim, J., Dinges, D.F., 2010. A meta-analysis of the impact of short-term sleep deprivation on cognitive variables. Psychol. Bull. 136, 375–389.
Lim, J., Tan, J.C., Parimal, S., Dinges, D.F., Chee, M.W.L., 2010a. Sleep deprivation impairs object-selective attention: a view from the ventral visual cortex. PLoS One 5, e9087.
Lim, J., Wu, W.C., Wang, J., Detre, J.A., Dinges, D.F., Rao, H., 2010b. Imaging brain fatigue from sustained mental workload: an ASL perfusion study of the time-on-task effect. NeuroImage 49, 3426–3435.
Mackworth, J.F., 1968. Vigilance, arousal, and habituation. Psychol. Rev. 75, 308–322.
Mandeville, J.B., Marota, J.J., Ayata, C., Moskowitz, M.A., Weisskoff, R.M., Rosen, B.R., 1999. MRI measurement of the temporal evolution of relative CMRO(2) during rat forepaw stimulation. Magn. Reson. Med. 42, 944–951.
Marois, R., Chun, M.M., Gore, J.C., 2000. Neural correlates of the attentional blink. Neuron 28, 299–308.
Mu, Q., Mishory, A., Johnson, K.A., Nahas, Z., Kozel, F.A., Yamanaka, K., Bohning, D.E., George, M.S., 2005. Decreased brain activation during a working memory task at rested baseline is associated with vulnerability to sleep deprivation. Sleep 28, 433–446.
Mumford, J.A., Hernandez-Garcia, L., Lee, G.R., Nichols, T.E., 2006. Estimation efficiency and statistical power in arterial spin labeling fMRI. NeuroImage 33, 103–114.
Ong, J.L., Asplund, C.L., Chia, T.T.Y., Chee, M.W.L., 2013. Now you hear me, now you don't: eyelid closures as an indicator of auditory task disengagement. Sleep (in press).
Parrish, T.B., Gitelman, D.R., LaBar, K.S., Mesulam, M.M., 2000. Impact of signal-to-noise on functional MRI. Magn. Reson. Med. 44, 925–932.
Paus, T., Zatorre, R.J., Hofle, N., Caramanos, Z., Gotman, J., Petrides, M., Evans, A.C., 1997. Time-related changes in neural systems underlying attention and arousal during the performance of an auditory vigilance task. J. Cogn. Neurosci. 9, 392–408.
Pelli, D.G., 1997. The VideoToolbox software for visual psychophysics: transforming numbers into movies. Spat. Vis. 10, 437–442.
Poudel, G.R., Innes, C.R.H., Jones, R.D., 2012. Cerebral perfusion differences between drowsy and nondrowsy individuals after acute sleep restriction. Sleep 35, 1085–1096.
Rao, H., 2012. ASL imaging of brain function changes during sleep restriction. Sleep 35, 1027–1028.
Schweickert, R., 1985. Separable effects of factors on speed and accuracy: memory scanning, lexical decision, and choice tasks. Psychol. Bull. 97, 530–546.
Shaw, T.H., Warm, J.S., Finomore, V., Tripp, L., Matthews, G., Weiler, E., Parasuraman, R., 2009. Effects of sensory modality on cerebral blood flow velocity during vigilance. Neurosci. Lett. 207–211.
Shen, Q., Ren, H., Duong, T.Q., 2008. CBF, BOLD, CBV, and CMRO(2) fMRI signal temporal dynamics at 500-msec resolution. Magn. Reson. Imaging 27, 599–606.
Smit, A.S., Eling, P.A.T.M., Coenen, A.M.L., 2004. Mental effort causes vigilance decrease due to resource depletion. Acta Psychol. (Amst) 115, 35–42.
Sternberg, S., 1969. The discovery of processing stages: extensions of Donders' method. Acta Psychol. (Amst) 30, 276–315.
Talairach, J., Tournoux, P., 1988. Co-planar Stereotaxic Atlas of the Human Brain. Thieme Medical Publishers, New York.
Temple, J.G., Warm, J.S., Dember, W.N., Jones, K.S., LaGrange, C.M., Matthews, G., 2000. The effects of signal salience and caffeine on performance, workload, and stress in an abbreviated vigilance task.
Thomas, M., Sing, H., Belenky, G., Holcomb, H., Mayberg, H., Dannals, R., Wagner, H., Thorne, D., Popp, K., Rowland, L., Welsh, A., Balwinski, S., Redmond, D., 2000. Neural basis of alertness and cognitive performance impairments during sleepiness. I. Effects of 24 h of sleep deprivation on waking human regional brain activity. J. Sleep Res. 9, 335–352.
Tomasi, D., Wang, R.L., Telang, F., Boronikolas, V., Jayne, M.C., Wang, G.J., Fowler, J.S., Volkow, N.D., 2009. Impairment of attentional networks after 1 night of sleep deprivation. Cereb. Cortex 19, 233–240.
Van Dongen, H.P.A., Belenky, G., Krueger, J.M., 2011. Investigating the temporal dynamics and underlying mechanisms of cognitive fatigue. In: Ackerman, P.L. (Ed.), Cognitive fatigue: multidisciplinary perspectives on current research and future applications. Decade of Behavior/Science Conference. American Psychological Association, Washington, DC USA, pp. 127–147.
Vul, E., Harris, C., Winkielman, P., Pashler, H., 2009. Puzzlingly high correlations in fMRI studies of emotion, personality, and social cognition.
Wang, J., Rao, H., Wetmore, G.S., Furlan, P.M., Korcykowski, M., Dinges, D.F., Detre, J.A., 2005. Perfusion functional MRI reveals cerebral blood flow pattern under psychological stress. Proc. Natl. Acad. Sci. U. S. A. 102, 17804–17809.
Warm, J.S., Parasuraman, R., Matthews, G., 2008. Vigilance requires hard mental work and is stressful. Hum. Factors 50, 433–441.
Wilkinson, R.T., 1964. Effects of up to 60 hours' sleep deprivation on different types of work. Ergonomics 7, 175–186.
Wong, E.C., Buxton, R.B., Frank, L.R., 1997. Implementation of quantitative perfusion imaging techniques for functional brain mapping using pulsed arterial spin labeling. NMR Biomed. 10, 237–249.
Wong, E.C., Buxton, R.B., Frank, L.R., 1998. A theoretical and experimental comparison of continuous and pulsed arterial spin labeling techniques for quantitative perfusion imaging. Magn. Reson. Med. 40, 348–355.
Wu, J.C., Gillin, J.C., Buchsbaum, M.S., Hershey, T., Hazlett, E., Sicotte, N., Bunney, W.E., 1991. The effect of sleep deprivation on cerebral glucose metabolic rate in normal humans assessed with positron emission tomography. Sleep 14, 155–162.
Wu, J.C., Gillin, J.C., Buchsbaum, M.S., Chen, P., Keator, D.B., Wu, N.K., Darnall, L.A., Fallon, J.H., Bunney, W.E., 2006. Frontal lobe metabolic decreases with sleep deprivation not totally reversed by recovery sleep. Neuropsychopharmacology 31, 2783–2792.